Published in final edited form as:
Mol Pharm. 2010 August 2; 7(4): 1301–1310. doi:10.1021/mp100089k.

Uptake, Distribution and Diffusivity of Reactive Fluorophores in Cells: Implications Toward Target Identification

Christopher W. Cunningham[†,◇,§], **Archana Mukhopadhyay**[‡,◇,§], **Gerald H. Lushington**[□], **Brian S. J. Blagg**[†,◇], **Thomas E. Prisinzano**[†,◇], and **Jeffrey P. Krise**[*,‡,◇]
Departments of Medicinal Chemistry and Pharmaceutical Chemistry, Molecular Graphics and Modeling Laboratory, and Specialized Chemistry Center, University of Kansas

Abstract

There is much recent interest in the application of copper-free click chemistry to study a wide range of biological events in vivo and in vitro. Specifically, azide-conjugated fluorescent probes can be used to identify targets which have been modified with bioorthogonal reactive groups. For intracellular applications of this chemistry, the structural and physicochemical properties of the fluorescent azide become increasingly important. Ideal fluorophores should extensively accumulate within cells, have even intracellular distribution, and be free (unbound), allowing them to efficiently participate in bimolecular reactions. We report here on the synthesis and evaluation a set of structurally diverse fluorescent probes to examine their potential usefulness in intracellular click reactions. Total cellular uptake and intracellular distribution profiles were comparatively assessed using both quantitative and qualitative approaches. The intracellular diffusion coefficients were measured using a fluorescence recovery after photobleaching (FRAP)-based method. Many reactive fluorophores exhibited suboptimal properties for intracellular reactions. BODIPY- and TAMRA-based azides had superior cellular accumulation, whereas TAMRA-based probes had the most uniform intracellular distribution and best cytosolic diffusivity. Collectively, these results provide an unbiased comparative evaluation regarding the suitability of azide-linked fluorophores for intracellular click reactions.

Keywords

Fluorescent dyes; tetramethylrhodamine; BODIPY; click chemistry; FRAP analysis; fluorescence microscopy

Introduction

One of the major hurdles associated with existing chemical target identification strategies occurs when the protein or proteins of interest exist in relatively low abundance in cells. In such cases, subsequent target isolation protocols are typically plagued with non-specific background binding, thus hindering separation and detection. Indeed, target identification

Corresponding Author Footnote: Department of Pharmaceutical Chemistry, 236B Simons Labs, Lawrence, KS 66045. Tel.: 785-864-2626; Fax: 785-864-5736. krise@ku.edu.
[†]Department of Medicinal Chemistry.
[‡]Department of Pharmaceutical Chemistry.
[□]Molecular Graphics and Modeling Laboratory.
[◇]Specialized Chemistry Center.
[§]These authors contributed equally to this work.

Supporting Information Available: Full characterization of fluorescent probes **1**–**12**. This information is available free of charge via the Internet at http://pubs.acs.org/.

has been called “the (often) missing link” in chemical genetics.[1–3] However, understanding the function of biomolecules is crucially dependent on observing them in their native environment in living cells.[4]

Chemical-based approaches have attempted to covalently modify drugs with fluorophores and reintroduce them back into cells to monitor their interactions with proteins in their native state.[5–7] The main limitation to this approach is that the resultant preassembled drug-fluorophore conjugate may be too large to readily diffuse across the plasma membrane of the cell, which would limit its ability to interact with cognate intracellular targets. Even if the drug-fluorophore complex can enter the cell, its intracellular distribution may be very different than that of the parent drug. Accordingly, the new conjugate may fail to sufficiently concentrate in the same intracellular localization as the parent drug, rendering results of intracellular protein target interactions difficult to interpret.

A method that has seen remarkable success in cellular tagging experiments involves the use of the copper-free click chemistry. There are numerous examples of bioorthogonal click reactions that were designed to label cell surface modified glycans,[8–9] and more recently in *in vivo* applications.[10–11] Azide-derivatized small molecules are able to react in copper-free conditions with several specially-designed bioorthogonal functional groups, including triarylphosphines *via* Staudinger ligation,[12–13] and gem-difluoro-cyclooctynes in alkyne-azide cycloaddition (AAC).[14] Using this methodology, we propose that azide-modified fluorescent tags can be highly attractive probe molecules for intracellular copper-free click chemistry applications.

In order to proceed with the development of strategies that employ intracellular click reactions for protein target identification purposes, it is important to identify fluorophores that have optimal cellular properties. We propose that ideal fluorophores for such an application should possess at least three important characteristics. First, the fluorophore should readily enter cells by passive diffusion and accumulate to a significant extent. The rate of the click reaction, being a bimolecular event, is proportional to the concentration of each of the components in the subcellular site of action. Accordingly, fluorophores with greater accumulation will have faster reaction rates and therefore have the highest potential to yield products that can be detected in a reasonable time frame for a cell-based phenotypic assay. Second, it is important that the fluorophore have relatively even intracellular distribution. This will allow the reactive fluorophore to reach its click partner regardless of the intracellular localization of the target. This is a significant concern considering that many small molecular weight molecules and drugs have been shown to specifically associate with distinct intracellular organelles or compartments.[15–19] Third, it is critical that the reactive fluorophore be free and available to react with the intended click partner once it is in the immediate vicinity of the target. Fluorophores that are tightly associated with membranes or abundant intracellular proteins will not be readily available to participate in the bimolecular reaction despite having good uptake and relatively even distribution. This can be determined quantitatively by measuring diffusion coefficients: fluorophores which are bound to cellular proteins show reduced diffusion coefficient values compared to non-bound fluorophores.

In this manuscript, we have comparatively evaluated the cellular uptake, distribution and diffusivity of a set of structurally diverse fluorophores using both qualitative and quantitative evaluations. We have used a normal human fibroblast cell line for these initial studies to generally establish the feasibility of performing click reactions using fluorescent probes. Collectively, these results provide a rational basis for the selection of fluorophores for applications in intracellular click reactions.

Experimental Section

Chemistry

The *N*-hydroxysuccinimidyl ester derivatives of fluorescent probes **1**–**3**, **5**–**12** were purchased from Molecular Probes (Eugene, OR) and Barry & Associates (**4**). Reagents were purchased from Sigma-Aldrich, Inc., and used without further purification. The ^{1}H NMR spectra were obtained using a Bruker Avance AV-III 500. TLC were performed on silica gel 60 GF plates (AnalTech, Inc., Newark, DE). Identity was determined using HRMS using an LCT Premier Mass Spectrometer. Analytical HPLC was carried out on an Agilent 1100 Series Capillary HPLC system with diode array detection at 254.8 nm on an Agilent Eclipse XDB-C18 column (4.6 × 150 mm, 5 μm).

Synthesis of Fluorescent Probes

General Procedure. The *N*-hydroxysuccinimide ester derivative of the appropriate fluorescent tag (2.0 mg) was added to a solution of 4-azido-1-butylamine (**13**) or 5-amino-1-pentanol (1.1 equiv.) and *N*,*N*-diisopropylethylamine (DIPEA, 1.1 equiv.) or triethylamine (NEt_3, 1.1 equiv.) in a solution of 10:1 dichloromethane/*N*,*N*-dimethylformamide (DCM/DMF, 1.0 mL). After stirring at RT for 3 hr under an atmosphere of Ar, the solution was partitioned between ethyl acetate/H_2O, the organic layer dried (Na_2SO_4), evaporated, and the product purified by column chromatography (silica gel, DCM/MeOH 95:5).

Cell culture and conditions

Normal human fibroblasts (CRL-2076) were cultured according the protocol provided from Coriell Cell Repository (Camden, NJ). Cells were cultured in a 5% CO_2 humidified atmosphere at 37°C in Dulbecco's Modified Eagle's Medium (DMEM, Invitrogen, Carlsbad, CA) supplemented with 10% fetal bovine serum (GIBCO-Invitrogen, Carlsbad, CA). Cells were maintained by passaging every fourth to fifth day by trypsinization with Trypsin/EDTA (Invitrogen, Carlsbad, CA). For microscopic images and FRAP analysis, cells were grown on cover strips to 75% confluency prior to experimentation.

Fluorescence Microscopy

Cells were incubated with 1μM fluorophore for 2 hours. After incubation, cells were washed with PBS to remove any unincorporated fluorophores. Images were taken using a Nikon Eclipse 80i microscope equipped for epifluorescence using the following filter sets: rhodamine (TAMRA, BODIPY-TMR analogues); FITC (Oregon Green); YFP (BODIPY-FL analogues); Texas Red (BODIPY-TR); GFP/FITC (Alexa Fluor 430, Cascade Yellow); GFP (diazaindacene); GFP/Em: 580/(±) 60 (PyMPO). For experiments that evaluated the intracellular distribution of fluorescent probes, a 60x objective was used and the microscope parameters, including fluorescence intensity and exposure, were optimized for each fluorophore. In comparative uptake experiments, a 60x objective was used and the fluorescence intensity and exposure time were held constant at 25% and 200 ms, respectively, for all fluorescent probes evaluated.

Calculation of Distribution Coefficient

1-Octanol/water distribution (logD) was determined using the shake-flask method in 1-octanol/buffer (pH 7.4) system.[16, 18] Briefly, 1-octanol and buffer (5 mM HEPES, 5 mM ammonium acetate, 5 mM KCl, 154 mM NaCl, pH 7.4) were pre-mixed in 1:4 1-octanol saturated buffer (Solution A) and 4:1 buffer saturated 1-octanol (Solution B) ratio by shaking gently at 220 rpm, 25°C for 24 hr. Thereafter, 5 μM stock solutions of test compound were prepared in pre-mixed Solution A or Solution B. Next, 500 μL of stock solution of the compound in Solution A is combined with 500 μL of Solution B in duplicate

Eppendorf tubes and mixed by gently shaking overnight. Reciprocal experiments using 500 μL of stock solution of compound in Solution B is combined with 500 μL of Solution A in duplicate Eppendorf tubes and mixed similarly. After shaking, Eppendorf tubes were centrifuged at 16×10^3 g for 10 min and 1-octanol and buffer layers were carefully removed in 100 μL to a 96 well plate. Standard curves for each compound were prepared from 5 nM to 5 μM in 1-octanol and buffer phases. The concentration of compound in both 1-octanol and buffer were determined from the standard curve by measuring fluorescence of test compound using a microplate fluorescence reader. The logD value of each compound was calculated from the logarithm of the ratio of the compound in 1-octanol and buffer phase.

Quantification of Cellular Uptake

Normal fibroblast cells were seeded in 6 well plates at the density of 500,000 cells per well. On the following day, cells were treated with the test compound to a final concentration of 2 μM for 2 hr. These conditions did not result in observable toxicity (blebbing, detachment from plates, etc). Following incubation, cells were collected, re-suspended in PBS and lysed with 250 μL lysis buffer (50 mM Tris HCl, 150 mM NaCl, 1% NP-40, pH 7.4). Cell lysate was then vortexed, 150 μL acetonitrile added, and centrifuged at 16,000 g for 15 min. The supernatant was used to measure the fluorescence of the compound using a microplate fluorescence reader. The extraction efficiency for each compound was determined separately and ranged from 55 to 85%. Extraction efficiency and standard curves for each compound were determined as described above over a range from 5 nM to 2 μM. Cellular uptake of the compound was determined from the extraction efficiency curve and normalized with protein concentration, which was determined using the BCA assay.

Intracellular Diffusion Constant Estimation

The diffusion constant of fluorescent probes was measured in cells using a previously described Fluorescence Recovery after Photobleaching (FRAP) technique.[20–21] Briefly, fibroblasts were treated with 2 μM of each test compound and incubated for 2 hr at 37°C, then washed with Hanks Balanced Salt Solution (HBSS, Invitrogen, Carlsbad, CA). The FRAP assay was performed using confocal laser microscopy on an upright LSM 510 laser microscope (Carl Zeiss, Thornwood, NY) equipped with a 63x oil-immersion objective lens. All bleaching experiments were performed with a defined circular spot using the 458–543 nm lines from a 4 mW Ar-ion laser operating at 50–100% of laser power. Unique photobleaching wavelengths were used for each fluorophore. A single iteration (200 per compound) was used for the bleach pulse, which lasted 11–86 s depending on compound and bleach spot size. After bleaching, fluorescence recovery was monitored at low laser intensity from 0.789–1.577 s intervals, depending on compound and bleaching spot.

ImageJ software was used to extract fluorescence intensity information from the bleached region as a function of time. A photobleach correction of the images was performed using the same circular spot area of a non-bleached region from the same cell. To correct any bleaching which might have occurred during collecting the stack of images, the values of fluorescence intensity of images post-bleach correction were normalized with the average intensity of the first 10 images before bleaching.[21]

Fluorescence recovery half life ($t_{1/2}$) was determined from curve fitting using inverse of exponential decay.[22] The diffusion coefficient is obtained by dividing the area of the photobleached region by the half-life for fluorescence recovery in that region.

Results

Synthesis and Physicochemical Evaluation of Reactive Fluorescent Probes

Derivatives of commercially-available fluorescent probes (Chart 1) were synthesized according to standard coupling methods shown in Scheme 1 (see Supplemental Material).[23] Known amino azide tethers were produced using a variation of known procedures,[24–25] specifically S_N2 displacement of alkyl bromide **13** with NaN_3, followed by phthalimide reduction using hydrazine hydrate in methanol in typical Gabriel deprotection fashion in high yield. Few hydrazide-reduced side products were seen, perhaps due to relatively short reaction time, dilute conditions, and low temperatures.

Fluorescent probes were selected to explore a range of molecular charge, lipophilicity, and polyfunctionality. We evaluated the influence of charge through the selection of fluorophores that are zwitterionic, anionic or neutral at physiologic pH. We purposely avoided the selection of fluorophores that are classified as weakly basic since they are have been previously shown to have non-uniform intracellular distribution. Specifically, such molecules have previously been shown to be sequestered in either acidic compartments such as lysosomes and the Golgi apparatus though an ion trapping-type mechanism[26–27] or into the mitochondria due to the net negative membrane potential associated with this compartment. Xanthene-based fluorophores, such as Oregon Green (**12**) and tetramethylrhodamine (TAMRA, **2** and **3**), contain carboxylate functional groups which are negatively charged at physiological pH. In the case of TAMRA, the *N*,*N*,*N'*,*N'*-tetramethylamino substituents also introduce a cationic charge, producing zwitterionic character in this backbone. Similarly, the 4-difluoro-4-bora-3a,4a-diaza-s-indacene (BODIPY) core of BODIPY-FL (**5** and **7**), BODIPY-TMR (**6** and **8**), and BODIPY-TR (**1**) contains a zwitterionic core which bears a localized anionic charge on a tetra-substituted boron atom, as well as a cationic charge delocalized throughout a tricyclic aromatic ring system. The pyridyloxazole family includes two derivatives, Cascade Yellow (**9**) and PyMPO (**10**), which are insensitive to cellular pH due to a cationic *N*-benzylpyridyl substituent. Cascade Yellow and Alexa Fluor 430 (**11**) were also selected for the presence of an aryl sulfonate group, which introduces anionic charge at physiological pH. Collectively, these fluorescent probes comprise multiple charge states, functional complexity, and fluorescence properties.

Molecular lipophilicity was another important variable that we sought to have widely represented in our set of fluorophores. Fluorescent probes contain functional groups which introduce charge and hydrogen bonding interactions which can influence their ability to interact with cellular membranes and proteins. We experimentally measured the $\log D_{pH7.4}$ for all probes using an octanol/water shake-flask partitioning assay, and the values ranged from −3.8 to 2.6 (see Table 1).

Finally, we sought to determine the potential influence of the azide moiety on the properties of the fluorophore. Although not charged at physiologically relevant pH, the azide could potentially interact with endogenous cellular proteins, which could result in changes in the intracellular distribution and diffusivity. To probe the influence of the azide, we have systematically replaced it with non-reactive alcohols.

Comparative Assessments of Total Cellular Accumulation

Reactive fluorophores should have adequate intracellular accumulation in order to enhance the rate of bimolecular intracellular click reactions. Total uptake of fluorophores was comparatively evaluated in cells using both qualitative and quantitative approaches. Qualitative cellular accumulation was determined by incubating cells with 2 μM fluorophore for two hours and immediately visualizing the cells using fluorescence microscopy.

Importantly, exposure time and lamp power were held constant for all of the captured images for comparison purposes. Representative micrographs of three of the azide-labeled fluorophores (**1**, **2** and **6**) are shown in Figure 2A. Overall, these qualitative evaluations were consistent with TAMRA and BODIPY-TR and -TMR azides having superior accumulation. Although such qualitative comparisons can give a relatively quick indication of relative uptake, several important factors exist that make accurately interpreting the results of these studies challenging. Differences in fluorescence quantum yields between fluorophores can make direct comparison difficult, and differences in photostability and fluorescence self-quenching reactions can make some fluorophores appear less concentrated, ultimately producing misleading results.[28–29]

To avoid these potential problems, we have analyzed the total cellular uptake using a quantitative approach. In this approach, we incubated cells with fluorophore-containing medium (2 mM for 2 hours). Following incubation, the cells were quickly washed and subsequently lysed. Untreated control cell lysates were spiked with known and varying amounts of each of the 12 fluorophores shown in Chart 1. Cellular extraction efficiencies and standard curves for each of the fluorophores were independently determined. Experimentally determined cell uptake values were obtained normalized to the amount of protein in the cell lysate (Figure 2B). Among the compounds analyzed, BODIPY-TR (**1**) and TAMRA (**2** and **3**) showed the highest uptake, whereas the lowest uptake seen with Oregon Green (**12**). The lipophilic BODIPY-TR (**1**) showed surprisingly high uptake compared with other BODIPY dyes (**5**–**8**). There was also no significant difference seen between alcohols and azides for TAMRA (**2** and **3**) and the BODIPY series (FL, **5** and **7**; TMR, **6** and **8**), further supporting the notion that this modification does not greatly influence cellular properties of fluorescent tags.

Evaluating the Intracellular Distribution of Fluorescent Probes

As previously discussed, optimal reactive fluorophores should extensively accumulate in cells to facilitate the rate of the intracellular bimolecular click reaction. However, substantial uptake alone is an insufficient indicator of a successful intracellular click reaction. Conceivably, a reactive fluorophore could extensively accumulate within a cell but would not engage in a click reaction due to compartmentalization in cellular organelles. Mammalian cells are extremely compartmentalized with over one half of the total cell volume comprised of membrane-bound organelles.[30] As target proteins can reside in one or in multiple compartments, it is imperative that the reactive fluorophore not only enters cells, but can reach intracellular targets regardless of their cellular localization.

Theoretically, small molecular weight molecules that passively diffuse across cell lipid bilayers should achieve uniform concentrations in all of the cellular compartments at steady state. This, however, is very rarely the case and most molecules have some degree on non-uniformity associated with their cellular distribution. Consistent with this observation, most of the evaluated fluorescent probes (**1**, **4**–**12**) exhibited non-uniform distribution throughout the cell, with many fluorophores showing little fluorescence within nuclear space (Figure 1). Fluorescent probes **2** and **3**, derivatives of the xanthene-based TAMRA fluorophore, showed even cellular distribution throughout the cytosol, and also permeate nuclear space to a large extent.

Molecules that show preferential nuclear accumulation are typically cationic and planar.[31] Interestingly, the quaternary amine-containing **10** has a net positive charge but does not show preferential nuclear staining. Considering the negative logD associated with this molecule, it is highly likely that it is not entering cells through passive diffusion. Instead, it would likely rely on endocytic uptake and would populate the early and late endosomes and lysosomes after a two hour incubation. Accordingly, this fluorophore is not able to reach the

nucleus. It is likely that other relatively hydrophilic fluorophores (i.e., **11** and **12**) are similarly taken up by fluid phase endocytosis and accumulate in endocytic compartments.

Several fluorophores appear to have relatively even cytosolic distribution but display apparent exclusion from the nucleus (see **1**, **5** and **11**, Figure 1). Although the nuclear membrane has numerous nuclear pore complexes (NPC) that allow small molecules (size < 5 kDa) to freely diffuse in and out of this compartment, the pore becomes restrictive to bulk flow when cytosolic molecules are greater than 30 kDa in size.[30] Accordingly, those fluorophores that show relatively even cytosolic distribution but appear to be restricted from the nucleus might be binding to soluble cytosolic macromolecules that are large enough to be restricted by the NPC. Another explanation for the apparent nuclear exclusion of these molecules could be due to the charge status of the fluorophore. As mentioned previously, cationic fluorophores are often drawn to the nucleus because of the high degree of negative charge associated with DNA.[31] Likewise, it is possible that fluorophores bearing a negative charge at physiological pH may be "excluded" from the nucleus through charge repulsion.

As seen in Figure 1, azide derivatives of TAMRA (**2**), BODIPY-FL-C_5 (**5**), and BODIPY-TMR (**6**) exhibit similar distribution patterns throughout the cytosol as their non-azide partners (**3**, **7**, and **8**, respectively). This indicates that this subtle functional change does not appreciably alter the cellular properties of fluorescent probes. Collectively, these results suggest that only TAMRA-based fluorophores seemingly have the propensity to distribute to an appreciable extent across the entire cell.

Measurement of Intracellular Diffusion Coefficients

Another, equally important property of the fluorophore has to do with its availability to participate in intracellular reactions with its intended click partner. Reactive fluorophores which extensively accumulate within the same intracellular compartment as the intended reactive target can still fail to undergo the desired click reaction if the fluorophore is strongly associated with cytosolic proteins or membranes. In order to efficiently participate in the bimolecular reaction, the reactive fluorophore must be free and not tightly associated with non-relevant endogenous molecules.

In an effort to evaluate this experimentally, we measured the diffusion coefficient of the fluorophore in the cells using a technique termed fluorescence recovery after photobleaching (FRAP).[20] The FRAP is a measure of the mobility of the fluorophore in the region of the cell that was bleached with high-intensity fluorescence excitation. Subsequently, the movement of un-bleached fluorophores that diffuse into the bleached area can be monitored. Using the area of the photobleach along with the measured half-life for recovery, one can arrive at the diffusion coefficient for the fluorophore in the cell. An example of the fluorescence intensity immediately after the photobleach and the resulting region of the cell 25 seconds after the photobleach is shown in Figure 3A. Plotting the fluorescence intensity in the bleached region as a function of time provides a kinetic plot that can be curve fit to determine the half-life for recovery (see Figure 3B). The resultant diffusion coefficients for all 12 fluorophores are shown in Table 1. Fluorophores **1**, **2** and **3** had diffusion coefficients that were much higher than all others evaluated (Figure 3C). All other fluorophores had very low diffusion coefficients that were considerably less than 0.5 μm^2/sec, suggesting that they may be strongly bound to endogenous macromolecules or membranes.

Discussion

There is much recent interest in catalyst-free click chemistry to study a wide variety of biological events.[14] Typically, one of the components of the click pair is labeled with a fluorophore or an affinity tag such as biotin to facilitate visualization. Initial applications of

click chemistry have been limited to extracellular proteins and glycolipids, and several recent studies have evaluated click reactions between cellular proteins and bioorthogonally conjugated probes.[14] In extracellular applications, the structural and physical attributes of the fluorophore- or biotin-conjugated click partner are not of great concern, considering that the reactive fluorophore does not need to cross biological barriers. For intracellular applications, however, the cellular permeability and intracellular distribution of the fluorescent azide probe are important considerations. It is likely that future applications of click chemistry will be increasingly directed toward the study of intracellular events and for protein target identification-type studies. Accordingly, a major challenge to this application will be the rational selection of reactive fluorophores that have optimal properties. We propose that there are three principal properties that a reactive fluorophore should possess in order to maximize its potential usefulness in intracellular applications and include: 1) the fluorophore should extensively accumulate within the cells; 2) the fluorophores should reach all intracellular organelles and compartments; and 3) the reactive fluorophore should not be extensively and tightly bound with endogenous molecules, therefore allowing it to interact with the target molecule of interest.

For many commercially available fluorophores, the uptake and intracellular distribution has not been extensively characterized. However, we and others have previously evaluated how structural and physicochemical properties of model compounds and drugs influence intracellular distribution.[15–16, 19] For example, many small molecular weight amine-containing molecules have the tendency to either accumulate in acidic intracellular compartments such as lysosomes or in the mitochondria.[17] Basic molecules with pKa values near 7 accumulate in organelles with acidic luminal pH, such as the lysosomes, late endosomes and Golgi, through an ion-trapping type mechanism. Noteworthy examples of such molecules include the Lysotracker class of fluorophores distributed by Molecular Probes (Invitrogen, Inc.). Alternatively, molecules that have very delocalized positive charges that are relatively membrane-permeable in their ionized form are preferentially sequestered into the mitochondria, due to the net negative membrane potential that is associated with these organelles.[32] We purposely avoided evaluating weakly basic fluorophores in this study considering their established propensity to have non-uniform cellular distribution.

Because drugs are known to distribute differently within different cell types, it is important to consider the choice of cell line while interpreting the results of this study. We selected a human fibroblast cell line because it consists of normal, non-transformed cells which have been well-characterized, leaving few variables to consider. Certain cancer cell lines, for example, have altered intracellular pH gradients which can modify probe distribution.[33] Others show up-regulated expression of multi-drug resistance (MDR) transporters, for which several xanthene-based fluorescent probes are known substrates.[34] One key example of this is P-glycoprotein (P-gp), a MDR transporter which is typically over-expressed in tumor cells and plays a significant role in the cellular uptake of a wide range of substrates, including xanthene-based fluorescent probes such as rhodamine 123 and fluorescein.[35] For these reasons, it is important to consider that some trends highlighted here may not hold for such vastly different cell types.

The compounds investigated in this manuscript had varying charge at physiological pH, which included molecules bearing a fixed positive charge (**10**), a negative charge (**12**), and zwitterionic (**2**, **3**, **5**–**9**, **11**). We also included one fluorophore (**4**) that had no ionizable functional groups. The predicted charge status of each of the fluorophores at pH 7 based upon reported or calculated pKa values are indicated on the structures in Figure 1.

Generally speaking, both membrane-permeable and membrane-impermeable molecules can significantly accumulate in cells, although by different mechanisms. Membrane-permeable molecules enter cells predominantly by passively diffusing across cellular lipid bilayers.[36] Alternatively, membrane-impermeable molecules rely on endocytic uptake and only populate endosomal and lysosomal compartments. Some molecules can have intermediate membrane permeability and therefore have contributions from both pathways. Although molecule can enter cells by both mechanisms, the capacity of cell accumulation is typically much greater for those molecules that utilize passive diffusion as opposed to endocytic uptake.

The octanol/buffer partition coefficient ($logD_{pH7.4}$) is a routine physicochemical measure of membrane permeability and it was experimentally determined for each of the fluorescent molecules evaluated in this study. As would be expected, the octanol/buffer partition coefficient showed a general correlation with total cell uptake (Figure 2). Specifically, very hydrophilic molecules with negative logD values had cellular accumulation much less than those with greater logD values. Compounds **10** and **12** (Figure 1) are examples of highly hydrophilic (low logD) fluorophores with low uptake and punctate fluorescence which appear to enter cells by endocytic uptake. Conversely, compounds such as **2** have high logD values and show high uptake into cells.

It is important to note that very high logD does not always translate into good cellular accumulation and distribution.[37] Very hydrophobic molecules typically have poor aqueous solubility. Moreover, such molecules can preferentially accumulate within the core of lipid bilayers. This may be the reason that compound **4**, despite having high logD, showed punctate intracellular localization, which could be caused by strong associations with organelle lipid bilayers.

There are other reasons that a fluorophore can have uneven intracellular distribution. For example, if a molecule binds with an endogenous organelle-resident molecule that is membrane-impermeable, the equilibrium will shifted to favor increased accumulation in that compartment because the free concentration of the molecule in the organelle is reduced due to the binding event. Practically speaking, such observations are typically observed with molecules that bind with DNA.[31] Molecules that show preferential nuclear accumulation are typically cationic and planar. This is the case for TAMRA derivatives **2** and **3** which have these properties and show some preferential nuclear association.

In addition to having good cellular uptake and even intracellular distribution, a reactive fluorophore should exist to a sufficient extent in its free unbound state to facilitate reactions with desired click partners. We propose that the magnitude of the diffusion coefficient of a reactive fluorophore inside a cell should correlate with its propensity to freely diffuse in the proximity of the target to allow productive chemical reactions to occur. There are two likely reasons that fluorophores have very low diffusion coefficients. One possibility is that the fluorophore is tightly associated with endogenous proteins (or protein complexes). If this occurs, the apparent size of the fluorophore will increase and the diffusion coefficient will be similar to that of the larger protein or protein complex to which the fluorophore is bound. Compounds **5** and **7** are examples of fluorophores with very low diffusivity (Figure 1). In addition, fluorophores that have very limited membrane-permeability that rely on endocytosis for cell uptake will remain trapped inside endocytic compartments. Fluorophores of this type will also have very low apparent diffusion coefficients considering that the fluorescence recovery would rely on trafficking of the unbleached organelles in into the bleached area. Obviously, this trafficking would be extremely slow relative to the diffusion of a protein or small molecule. One example is compound **12**, which is highly

hydrophilic and has punctate fluorescence. Regardless of the precise reason, molecules with very low diffusion coefficients will not be optimal for applications in intracellular reactions.

Whether or not a fluorophore significantly accumulates within the nucleus can provide important clues regarding its potential suitability in intracellular click reactions, even if the target is not located in the nucleus. Molecules of less than 30 kDa in size are thought to freely permeate across the highly abundant nuclear pore complexes (NPC) and enter the nucleoplasm. There are two likely reasons that a small molecular weight fluorophore would fail to accumulate in the nucleus. For anionic molecules, the lack of nuclear association could be due to charge repulsion with anionic DNA molecules. This is likely the case with **11**, the only fluorophore bearing a net negative charge at physiological pH. However, it is interesting that **1** is apparently excluded from the nucleus despite the fact that it bears no net negative charge. In this case, it is likely that **1** is significantly bound with a cytosolic protein that is greater than 30 kDa in size, thus restricting its diffusion into the nucleus. The fact that the diffusion coefficient for **1** is significantly less than TAMRA-based fluorophores **2** and **3** is consistent with this possibility.

Collectively, our results suggest that TAMRA-based fluorophore **2** had superior combination of uptake, intracellular distribution and diffusivity compared to all other fluorophores tested. Interestingly, our results predicting the superior suitability of the TAMRA-based reactive fluorophores has been demonstrated by Salic and Mitchison.[38] The purposes of the studies disclosed here is to identify the fluorescent probes which exhibit the optimal cellular properties for intracellular [3+2] click chemistry applications. As an initial proof-of-principle, we have repeated the initial example of intracellular click chemistry disclosed by Salic and Mitchison (Figure 4). Using fibroblast cells with DNA modified with the click-reactive, alkyne-derived nuclear base 5-ethynyl-2′-deoxyuridine (EdU, Berry & Associates) and unmodified, non-reactive thymidine controls, we are able to see evidence of covalent conjugation of TAMRA azide (**3**) within the nuclei of click-modified cells (Figure 4, Panel A), but not within control cells (Figure 4, Panel B). Future studies will be performed which aim to quantitate the efficiency of the [3+2] click reaction for the fluorophores described here. Taken together, membrane-permeable fluorescent probe selection plays a substantial role in the success of intracellular “click” cyclization reactions.

Supplementary Material

Refer to Web version on PubMed Central for supplementary material.

Acknowledgments

The authors thank Dr. Jeffrey Aubé for all of his input and helpful discussions throughout the project, as well as Dr. Justin Douglas and Sarah Neuenswander for assistance with NMR experiments and Dr. Bernard Wiredu for his contributions to the project. We thank David Moore (Microscopy and Analytical Imaging Laboratories, University of Kansas) for help with FRAP analysis, and Ryan S. Funk and Damon T. Jacob for their assistance with fluorescence microscopy image analysis. We are grateful to the NIH for financial support (5U54 HG005031).

References

1. Burdine L, Kodadek T. Target identification in chemical genetics: the (often) missing link. Chem Biol. 2004; 11(5):593–597. [PubMed: 15157870]
2. Peddibhotla S, Dang Y, Liu JO, Romo D. Simultaneous arming and structure/activity studies of natural products employing O-H insertions: an expedient and versatile strategy for natural products-based chemical genetics. J Am Chem Soc. 2007; 129(40):12222–12231. [PubMed: 17880073]
3. Inverarity IA, Hulme AN. Marked small molecule libraries: a truncated approach to molecular probe design. Org Biomol Chem. 2007; 5(4):636–643. [PubMed: 17285172]

4. Fokin VV. Click imaging of biochemical processes in living systems. ACS Chem Biol. 2007; 2(12): 775–778. [PubMed: 18154263]
5. Johnsson N, Johnsson K. Chemical tools for biomolecular imaging. ACS Chem Biol. 2007; 2(1):31–38. [PubMed: 17243781]
6. Rao J, Dragulescu-Andrasi A, Yao H. Fluorescence imaging in vivo: recent advances. Curr Opin Biotechnol. 2007; 18(1):17–25. [PubMed: 17234399]
7. Sadaghiani AM, Verhelst SH, Bogyo M. Tagging and detection strategies for activity-based proteomics. Curr Opin Chem Biol. 2007; 11(1):20–28. [PubMed: 17174138]
8. Baskin JM, Prescher JA, Laughlin ST, Agard NJ, Chang PV, Miller IA, Lo A, Codelli JA, Bertozzi CR. Copper-free click chemistry for dynamic in vivo imaging. Proc Natl Acad Sci U S A. 2007; 104(43):16793–16797. [PubMed: 17942682]
9. Agard NJ, Prescher JA, Bertozzi CR. A strain-promoted [3 + 2] azide-alkyne cycloaddition for covalent modification of biomolecules in living systems. J Am Chem Soc. 2004; 126(46):15046–15047. [PubMed: 15547999]
10. Laughlin ST, Bertozzi CR. In vivo imaging of Caenorhabditis elegans glycans. ACS Chem Biol. 2009; 4(12):1068–1072. [PubMed: 19954190]
11. Laughlin ST, Baskin JM, Amacher SL, Bertozzi CR. In vivo imaging of membrane-associated glycans in developing zebrafish. Science. 2008; 320(5876):664–667. [PubMed: 18451302]
12. Prescher JA, Dube DH, Bertozzi CR. Chemical remodelling of cell surfaces in living animals. Nature. 2004; 430(7002):873–877. [PubMed: 15318217]
13. Chang PV, Prescher JA, Hangauer MJ, Bertozzi CR. Imaging cell surface glycans with bioorthogonal chemical reporters. J Am Chem Soc. 2007; 129(27):8400–8401. [PubMed: 17579403]
14. Sletten EM, Bertozzi CR. Bioorthogonal chemistry: fishing for selectivity in a sea of functionality. Angew Chem Int Ed Engl. 2009; 48(38):6974–6998. [PubMed: 19714693]
15. Gong Y, Duvvuri M, Krise JP. Separate roles for the Golgi apparatus and lysosomes in the sequestration of drugs in the multidrug-resistant human leukemic cell line HL-60. J Biol Chem. 2003; 278(50):50234–50239. [PubMed: 14522995]
16. Duvvuri M, Gong Y, Chatterji D, Krise JP. Weak base permeability characteristics influence the intracellular sequestration site in the multidrug-resistant human leukemic cell line HL-60. J Biol Chem. 2004; 279(31):32367–32372. [PubMed: 15181006]
17. Duvvuri M, Krise JP. Intracellular drug sequestration events associated with the emergence of multidrug resistance: a mechanistic review. Front Biosci. 2005; 10:1499–1509. [PubMed: 15769640]
18. Duvvuri M, Konkar S, Funk RS, Krise JM, Krise JP. A chemical strategy to manipulate the intracellular localization of drugs in resistant cancer cells. Biochemistry. 2005; 44(48):15743–15749. [PubMed: 16313177]
19. Rosania GR. Supertargeted chemistry: identifying relationships between molecular structures and their sub-cellular distribution. Curr Top Med Chem. 2003; 3(6):659–685. [PubMed: 12570858]
20. Sprague BL, Pego RL, Stavreva DA, McNally JG. Analysis of binding reactions by fluorescence recovery after photobleaching. Biophys J. 2004; 86(6):3473–3495. [PubMed: 15189848]
21. Braeckmans K, Peeters L, Sanders NN, De Smedt SC, Demeester J. Three-dimensional fluorescence recovery after photobleaching with the confocal scanning laser microscope. Biophys J. 2003; 85(4):2240–2252. [PubMed: 14507689]
22. Sprague BL, McNally JG. FRAP analysis of binding: proper and fitting. Trends Cell Biol. 2005; 15(2):84–91. [PubMed: 15695095]
23. Mottram LF, Maddox E, Schwab M, Beaufils F, Peterson BR. A concise synthesis of the Pennsylvania Green fluorophore and labeling of intracellular targets with O6-benzylguanine derivatives. Org Lett. 2007; 9(19):3741–3744. [PubMed: 17705395]
24. Varghese S, Gupta D, Baran T, Jiemjit A, Gore SD, Casero RA Jr, Woster PM. Alkyl-substituted polyaminohydroxamic acids: a novel class of targeted histone deacetylase inhibitors. J Med Chem. 2005; 48(20):6350–6365. [PubMed: 16190761]

25. Karle M, Bockelmann D, Schumann D, Griesinger C, Koert U. Conformative coupling of two conformational molecular switches. Angew Chem Int Ed Engl. 2003; 42(37):4546–4549. [PubMed: 14520763]
26. de Duve C, de Barsy T, Poole B, Trouet A, Tulkens P, Van Hoof F. Commentary. Lysosomotropic agents. Biochem Pharmacol. 1974; 23(18):2495–2531. [PubMed: 4606365]
27. Chou KM, Paul Krapcho A, Hacker MP. Impact of the basic amine on the biological activity and intracellular distribution of an aza-anthrapyrazole: BBR 3422. Biochem Pharmacol. 2001; 62(10): 1337–1343. [PubMed: 11709193]
28. Duvvuri M, Feng W, Mathis A, Krise JP. A cell fractionation approach for the quantitative analysis of subcellular drug disposition. Pharm Res. 2004; 21(1):26–32. [PubMed: 14984254]
29. Arbeloa FL, Ojeda PR, Arbeloa IL. Fluorescence self-quenching of the molecular forms of Rhodamine B in aqueous and ethanolic solutions. J Lumines. 1989; 44:105–112.
30. Alberts, B.; Bray, D.; Lewis, JW.; Raff, M.; Roberts, K.; Watson, JD. Intracellular sorting and the maintenance of cellular compartments. In: Robertson, M., editor. Molecular Biology of the Cell. 2. Garland Publishing, Inc; New York, NY: 1989. p. 405-479.
31. Lansiaux A, Dassonneville L, Facompre M, Kumar A, Stephens CE, Bajic M, Tanious F, Wilson WD, Boykin DW, Bailly C. Distribution of furamidine analogues in tumor cells: influence of the number of positive charges. J Med Chem. 2002; 45(10):1994–2002. [PubMed: 11985467]
32. Rashid F, Horobin RW. Interaction of molecular probes with living cells and tissues. Part 2. A structure-activity analysis of mitochondrial staining by cationic probes, and a discussion of the synergistic nature of image-based and biochemical approaches. Histochemistry. 1990; 94(3):303–308. [PubMed: 1698190]
33. Duvvuri M, Konkar S, Hong KH, Blagg BS, Krise JP. A new approach for enhancing differential selectivity of drugs to cancer cells. ACS Chem Biol. 2006; 1(5):309–315. [PubMed: 17163760]
34. Gong Y, Duvvuri M, Duncan MB, Liu J, Krise JP. Niemann-Pick C1 protein facilitates the efflux of the anticancer drug daunorubicin from cells according to a novel vesicle-mediated pathway. J Pharmacol Exp Ther. 2006; 316(1):242–247. [PubMed: 16174794]
35. Sun H, Miller DW, Elmquist WF. Effect of probenecid on fluorescein transport in the central nervous system using in vitro and in vivo models. Pharm Res. 2001; 18(11):1542–1549. [PubMed: 11758761]
36. Walter A, Gutknecht J. Permeability of small nonelectrolytes through lipid bilayer membranes. J Membr Biol. 1986; 90(3):207–217. [PubMed: 3735402]
37. Acharya C, Seo PR, Polli JE, MacKerell AD Jr. Computational model for predicting chemical substituent effects on passive drug permeability across parallel artificial membranes. Mol Pharm. 2008; 5(5):818–828. [PubMed: 18710255]
38. Salic A, Mitchison TJ. A chemical method for fast and sensitive detection of DNA synthesis in vivo. Proc Natl Acad Sci U S A. 2008; 105(7):2415–2420. [PubMed: 18272492]
39. Haugland, RP. Handbook of Fluorescent Probes and Research Products. In: Gregory, J., editor. Probes for Organelles. 8. Molecular Probes, Inc; Eugene, OR: 2001.

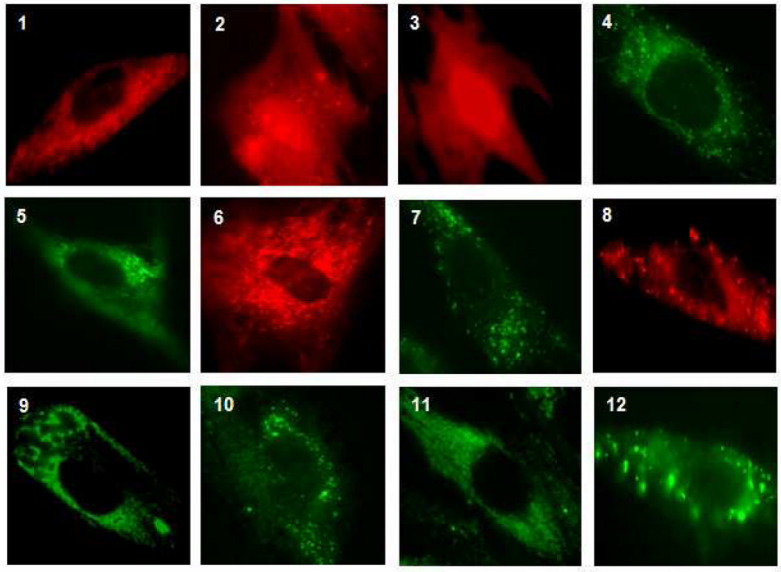

Figure 1.

Fluorescence microscopy images for probes **1**–**12**. Cells were incubated with 1μM fluorophore for 2 hours, then washed with PBS to remove any unincorporated fluorophores. Images were taken using a Nikon Eclipse 80i microscope equipped for epifluorescence using filter sets as described in the Experimental Section. A 60x objective was used and the microscope parameters, including fluorescence intensity and exposure, were optimized for each fluorophore.

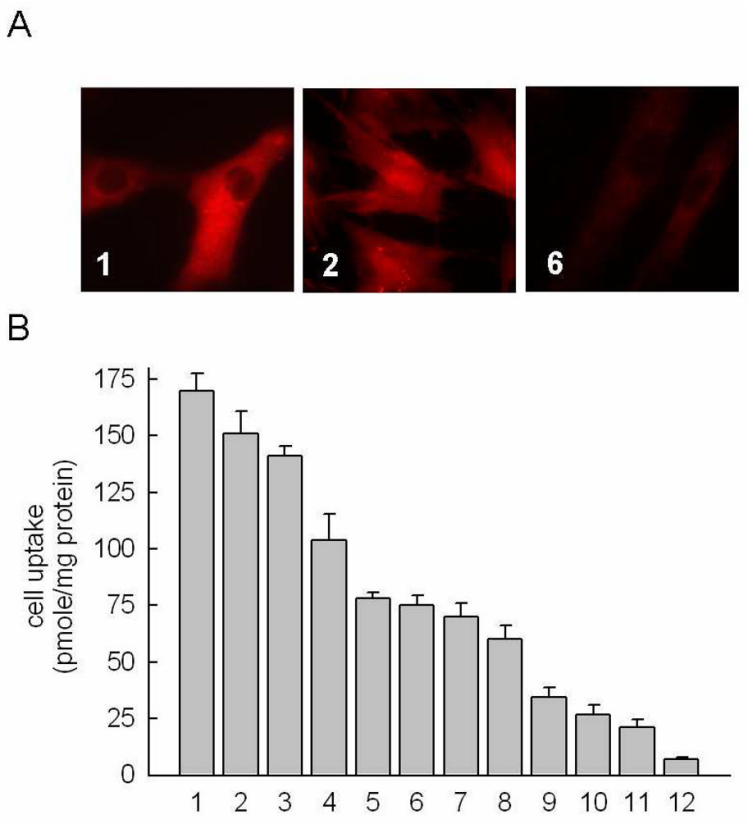

Figure 2.

A) Qualitative comparison of fluorescence microscopy images of **1**, **2**, and **6**. Fluorescence images were taken using conditions as described in the Experimental section. B) Quantitative comparison of cellular uptake for **1**–**12**. Cells were treated with the test compound to a final concentration of 2 μM for 2 hr before evaluation. Cellular uptake of each compound was determined and normalized to protein concentration in the sample.

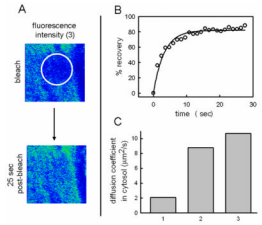

Figure 3.

Results of FRAP assays. A) Fluorescence images immediately following photobleaching (top) and 25 s post-bleach period (bottom) for probe **3**. B) Correlation plot of % fluorescence recovery as a function of time for probe **3**. C) Diffusion coefficient values for probes **1**–**3**. The diffusion coefficient is obtained by dividing the area of the photobleached region by the half-life for fluorescence recovery in that region. The diffusion coefficients for probes 4-12 are not included on the graph and were all less than 0.5 $\mu m^2/s$.

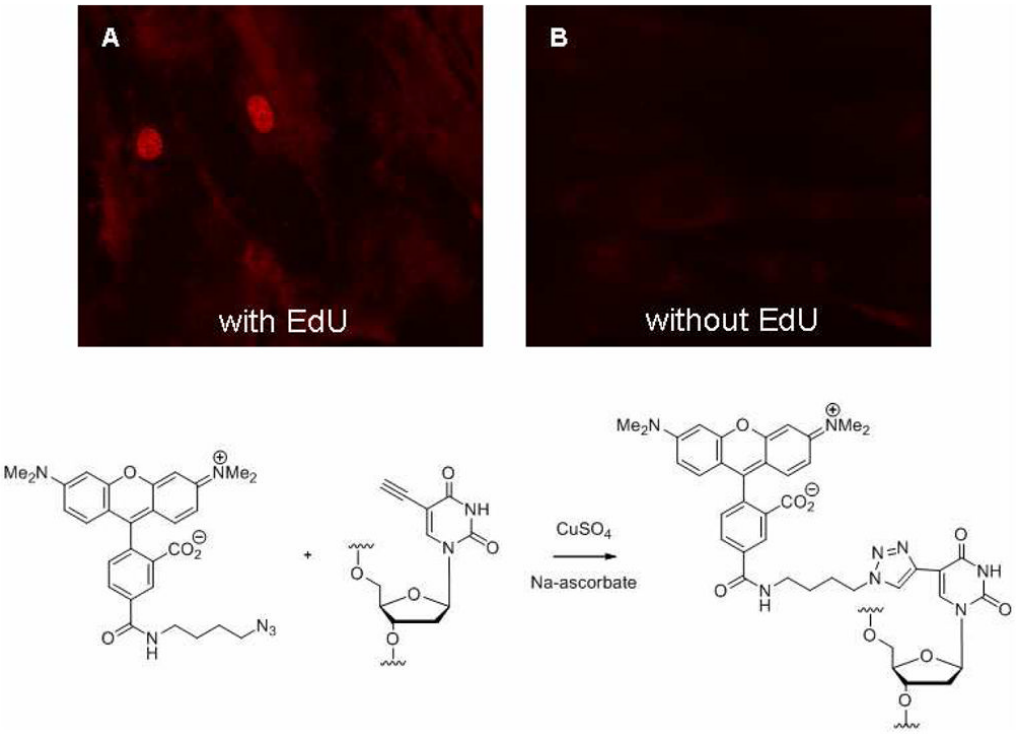

Figure 4.

Click chemistry within cells. The modified thymidine derivative 5-ethynyl-2′-deoxyuridine (EdU, Berry & Associates) was incorporated into DNA of normal human fibroblast cells according to the method described in Reference [38]. Fibroblast cells which were not treated with EdU were used as a negative control. Cells were then pre-incubated with TAMRA-N_3 (**3**, 1μM) for 3 hr before treatment with $CuSO_4$ (0.5 mM) and ascorbic acid (100 mM) for 15 min. Following that, cells were quick washed several times to remove any unbound fluorophore. Live cell images of cells which had been modified with EdU (Panel A) showed a large degree of nuclear staining, indicating covalent attachment of the fluorescent probe with DNA. This was not seen with control cells that did not incorporate alkynes (Panel B).

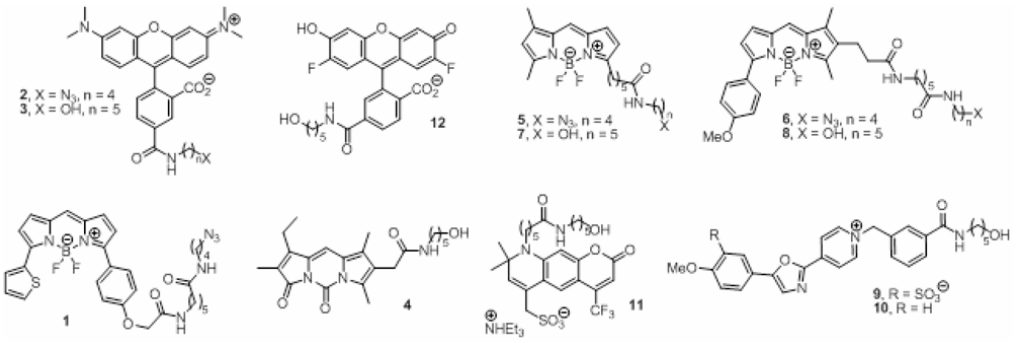

Chart 1.
Structures of Fluorescent Probes **1**–**12**.

Table 1

Physical Properties of Fluorescent Probes **1**–**12**.

		Fluorescence (λ, nm)[a]				
Cpd ID	**Common Name**	**Ex.**	**Em.**	**MW (Da)**	**$logD_{pH\ 7.4}$[b]**	**Diffusion Coefficient (D, μm²/s)**
1	BODIPY-TR-N_3	588	617	633.52	0.88	2.1
2	TAMRA-N_3	555	580	554.65	2.6	8.8
3	TAMRA-OH	555	580	510.61	0.3	10.8
4	Diazaindacene-OH	425[c]	535[c]	399.48	4.1	< 0.5
5	BODIPY-FL-C_5-N_3	504	513	416.28	2.5	< 0.5
6	BODIPY-TMR-N_3	535	574	607.50	1.5	< 0.5
7	BODIPY-FL-C_5-OH	504	513	405.29	1.3	< 0.5
8	BODIPY-TMR-OH	535	574	596.52	1.4	< 0.5
9	Cascade Yellow-OH	409	558	551.62	−1.25	< 0.5
10	PyMPO-OH	410	570	552.46	−0.15	< 0.5
11	Alexa Fluor 430-OH	430	545	689.83	−1.38	< 0.5
12	Oregon Green-OH	496	524	497.41	−3.8	< 0.5

[a] Data courtesy of Molecular Probes,[39] unless otherwise noted.

[b] Determined experimentally (see Methods Section).

[c] Data courtesy of Barry & Associates.